NBSIR 78-869

ERROR EQUATIONS USED IN THE NBS EARTH TERMINAL MEASUREMENT SYSTEM

William C. Daywitt

Electromagnetics Division
Institute for Basic Standards
National Bureau of Standards
Boulder, Colorado 80302

December 1977

NBSIR 78-869

ERROR EQUATIONS USED IN THE NBS EARTH TERMINAL MEASUREMENT SYSTEM

William C. Daywitt

Electromagnetics Division
Institute for Basic Standards
National Bureau of Standards
Boulder, Colorado 80302

December 1977

U.S. DEPARTMENT OF COMMERCE, Juanita M. Kreps, Secretary
Sidney Harman, Under Secretary
Jordan J. Baruch, Assistant Secretary for Science and Technology

NATIONAL BUREAU OF STANDARDS, Ernest Ambler, Acting Director

CONTENTS

LIST OF FIGURES AND TABLES

ERROR EQUATIONS USED IN THE NBS EARTH TERMINAL MEASUREMENT SYSTEM

William C. Daywitt

An outline for the derivation of equations employed in a measurement and error analysis of satellite EIRP using a calibrated radio star is presented. A table showing analysis results at 7.55 GHz using Cassiopeia A for a satellite at 12° elevation angle is given. The quadrature sum of the systematic errors appearing in the table is 10.1%. Also presented is a curve of the systematic errors as a function of elevation angle showing a 7.3% minimum at high elevation angles. Included are working equations for the calculation of correction and errors.

Key Words: C/kT; EIRP; error analysis; G/T; precision measurements; radio star, satellite communications.

I. INTRODUCTION

The National Bureau of Standards has constructed a system designed to measure satellite EIRP using a calibrated radio star. The system operates off the i-f patch panel of the downlink earth terminal (ET), and automatically controls the several measurement sequences.

The method employed in the earth-terminal measurement system (ETMS) is a modified version of the radio-star method [1] of measuring satellite EIRP (effective isotropic radiated power), the modification [2] allowing ET receiver gain fluctuations to be removed from the measurement, significantly reducing measurement error.

In addition to a digital voltmeter and accurately calibrated i-f attenuators, the ETMS features a very accurate power bridge [3], and an improved solid-state noise source [4] of high stability. Combined, the components can routinely measure power ratios to a few hundreths of a decibel. The ETMS also incorporates well calibrated i-f bandpass filters whose characteristics are combined with the observed ET passband characteristics by the computer software in the ETMS to obtain the overall noise bandwidth needed for the calculation of EIRP.

A measurement and error analysis for the 1 to 10 GHz frequency range to be reviewed in this paper is incorporated in the ETMS computer software. The analysis reveals additional errors and a higher atmospheric correction than previously calculated.

The relationship of the ETMS to the ET receiving system is shown in figure 1. The receiving system is represented by the ET antenna, cross-guide coupler, low-noise amplifier (LNA), downconverter, and i-f patch panel. The ETMS consists of the solid-state noise source, and the power measurement and control console. The noise source is connected to the receiving system through the cross-guide coupler, and T_a is the noise temperature representing the noise power added to the system at the LNA when the noise source is turned on. The gain of the system from the antenna far-field to the LNA is represented by G, and is the product of the antenna gain and the waveguide loss from the antenna to the LNA.

The noise source serves a double purpose in the EIRP measurement. The first is to eliminate gain fluctuations [2] from the LNA input to the power detector in the ETMS. This is accomplished by performing all power measurements in pairs, one measurement with the

noise source turned off, followed immediately by the same measurement with the noise source turned on. The noise-source-off measurement is then normalized by the difference between the two measurements, thus eliminating the system gain (and consequently the possibility of gain fluctuations) between the LNA and the ETMS power detector from the power ratio. Besides the immediate benefit of removing these short-term gain fluctuations, measurements may now be accurately compared on a day-to-day basis. The second purpose is to provide a calibratable source of power by which the magnitude of the received satellite signal power can be measured. The calibration of this noise power is accomplished in the first step of the EIRP measurement by comparing the reduced noise temperature (T_a/G) of the noise source against the power from a calibrated radio star.

The EIRP measurement method employed by the ETMS involves two steps: 1) A radio-star calibration of the reduced noise temperature (T_a/G) of the solid-state noise source as a function of ET antenna elevation angle; and 2) the measurement of the available powers at the LNA input received from the satellite. The first step is performed by measuring the i-f power from the ET receiving system as the radio star drifts through the mainbeam of the antenna. These measurements are performed at various elevation angles as the star traverses its path across the sky, and yield a set of T_a/G data points as depicted in figure 2. The least-squares curve fit to these data points represents a calibration curve for the "front-end" of the receiving system, and the solid-state noise source. The 6.5% value appearing in the figure represents random scatter (1σ) of the data points. The curve remains valid as long as T_a and G remain constant in time. Measurements performed on the noise source [4] show it to be stable to within ± 0.01 dB (1σ) over at least the time required to complete a set of EIRP measurements for a number of frequencies. The gain G is assumed to remain constant for this same period, an assumption that appears to be born out by experience. Once the calibration curve is established, the value of T_a/G for any satellite elevation angle can be easily determined by reading the value of T_a/G from the curve at that angle.

After obtaining the T_a/G calibration curve, the ET antenna is pointed at the satellite whose EIRP is to be measured, and a number of measurements of received satellite power are performed. The average of these measurements normalized by T_a yields a ΔY that can be used with the proper (at the satellite elevation angle) T_a/G value to determine the satellite EIRP from the equation

$$EIRP = \frac{k(T_a/G)\ \ \Delta f\ L\ \Delta Y}{A\ e_1 \cdots e_7} \qquad (1)$$

where k is Boltzmann's constant, Δf is the combined ET-ETMS noise bandwidth, L is the space loss $(4\pi r/\lambda)^2$ [5], r is the range from the ET antenna to the satellite transmit antenna, λ is the measurement wavelength, and A is the aspect angle correction [1]. e_1 through e_7 are near-unity correction factors analogous to the G/T correction factors described in an earlier publication [6]. Sequentially, these factors account for: 1) Atmospheric transmission losses; 2) the angular extent of the received satellite signal as "seen" by the ET antenna; 3) frequency variations of the receiving system components across the receiver passband; 4) frequency variations of the downlink operating noise temperature across the receiver

passband; 5) imperfect ET antenna pointing; 6) polarization mismatch between satellite signal and ET antenna; and 7) finite response time of the ETMS and instabilities in T_a.

The theoretical development leading to equation (1) is outlined in the next section.

II. THEORETICAL DEVELOPMENT

As mentioned earlier the EIRP measurement performed by the ETMS is accomplished in two steps, obtaining the T_a/G calibration curve, and measuring the received satellite power. Before examining these two steps separately, basic equations used as a starting point for their theoretical descriptions will be presented. Although these equations and some of the approximations leading to the final working equations may be applicable over a wider frequency range, they are designed primarily for the 1 to 10 GHz frequency range.

A model of the ET receiving system is shown in the block diagram of figure 3. The system (including the atmosphere) is outlined in solid blocks. The far-field source is the satellite or radio star, depending at which the ET antenna is pointed, and $B(\Omega,f)$ is the corresponding brightness distribution [7]. Ω represents the pair of spherical polar angles with origin at the ET antenna and z-axis along the center of the mainbeam, and f is the frequency. $\alpha(\Omega,f)$ is an operator representing the effects [8,6] of gaseous absorption, refractive spreading, and tropospheric scattering on the incoming flux from the radio star or satellite. $M(f)$ is a mismatch factor [9] relating the polarization of the source radiation to the ET antenna polarization. $A_e(f)$ and $G(f)$ are the effective area and gain respectively of the combined antenna, waveguide feed, and cross-guide coupler. $T_a(f)$ is the noise temperature of the solid-state noise source as it appears at the LNA input. When the noise source is turned off, the added noise $T_a(f)$ is zero. $T(f)$ is the noise temperature of the ET system and consists of cosmic background noise; atmospheric and man-made noise; ground noise; noise from I^2R losses in the antenna, waveguide feed, and cross-guide coupler; the effective input noise temperature of the LNA; and radiated satellite noise when the ET antenna is pointed at the satellite. $w(f)$ is the spectral power (power per unit bandwidth) corresponding to the sum of the spectral power from the far-field source, $kT_a(f)$, and $kT(f)$. $g(f)$ is the ratio of the spectral power delivered to the power meter to the available spectral power at the LNA input. P is the total power delivered to the power meter.

The spectral power $w(f)$ is related to other parameters appearing in figure 3 by the equation

$$w(f) = k[T(f) + "T_a(f)"] + A_e(f)M(f) \int \alpha(\Omega,f)B(\Omega,f)\cdot P_n(\Omega-\Omega_o,f)\ d\Omega. \qquad (2)$$

$P_n(\Omega-\Omega_o,f)$ is the normalized power pattern of the ET antenna, waveguide feed, cross-guide coupler comibination, where the difference $\Omega-\Omega_o$ accounts for the fact that the antenna may not be pointing at the center Ω_o of the far-field source. The quotation marks around $T_a(f)$ are a reminder that $T_a(f)$ is zero when the solid-state noise source is turned off. $d\Omega$ is the infinitesimal solid angle $\sin\theta\ d\theta\ d\psi$.

The power P detected by the ETMS is related to the spectral power w(f) by the equation

$$P = \int w(f)g(f)df \ . \tag{3}$$

The form of equations (2) and (3) are a manifestation of the assumed linearity of the model in figure 3, and form the theoretical basis for the following description of the two-step measurement process leading to the EIRP equation (1).

A. Step One - T_a/G Calibration Curve

The power measurements performed by the ETMS to obtain T_a/G at a particular elevation angle are indicated by the heavy dots in figure 4. As a calibrated radio star passes through the center of the ET antenna mainbeam, the i-f power detected by the ETMS describes a curve shaped somewhat as depicted in the figure. The slope of the baseline from t_1 to t_3 could be caused by a variation in the cosmic background surrounding the radio star, or a slow change in the ET receiver gain. Three pairs of power measurements are made, one at each time t_1, t_2, and t_3. At t_1 a measurement P_1 of the noise baseline is made, followed immediately by the same measurement $P_1 + P_a$ with the solid-state noise source turned on. As previously described, the ratio y_1 (= P_1/P_a) is then calculated to eliminate the receiver gain from consideration. Similar ratios y_2 (= P_2/P_a) and y_3 (= P_3/P_a) are calculated from measurements at t_2 and t_3. The measurement at t_2 corresponds to the radio star being in the center of the ET antenna pattern. The measurement at t_3 is another measurement of the noise baseline and which, with y_1, allows the value of the noise baseline at t_2 to be determined. By subtracting the noise baseline from the measurement at t_2 the i-f power ratio difference Δy corresponding to the radio star can be determined from the equation

$$\Delta y = y_2 - (y_1 + y_3)/2 \tag{4}$$

The values of the measured powers in figure 4 can be related to the quantities in the block diagram of figure 3 through equations (2) and (3). For example,

$$P_2 = \int g(f)[kT(f) + A_e(f)M(f) \int B(\Omega,f)\alpha(\Omega,f)P_n(\Omega,f)d\Omega]df \tag{5}$$

and

$$P_a = \int g(f)kT_a(f)df \ . \tag{6}$$

The $B(\Omega,f)$ in equation (5) is the radio-star brightness distribution, and M(f) (approximately equal to 1/2) is the corresponding mismatch factor.

Equations (5) and (6) with similar equations for the measurements at t_2 and t_3 can be combined to give a theoretical expression for the Δy of equation (4). When this is done and equated to Δy the following equation can be derived

$$\frac{T_a}{G} = \frac{\lambda^2 S}{8\pi k} \cdot \frac{k_1 \cdots k_7}{\Delta y} \ . \tag{7}$$

λ is the measurement wavelength, $S = B(\Omega,f)d\Omega$ is the radio-star flux density at frequency f, and k is again Boltzmann's constant. k_1 through k_7 are correction factors defined to give the functional form of equation (7), and are complicated expressions containing a number of integrals. Under certain circumstances these factors are close to unity, making accurate radio-star measurements of G/T or EIRP possible. Reduced expressions for the k_i's have been discussed in an earlier publication [6], and are presented in the Appendix.

The value for T_a/G calculated from equation (7) pertains to a particular elevation angle. When this process is repeated for other elevation angles as the radio-star traverses its path across the sky, the data points in figure 2 from which the calibration curve is derived, are generated. The T_a/G value need to determining the satellite signal power is then obtained from the curve at the elevation angle of the satellite.

B. Step Two - Received Satellite Power Measurements

With the T_a/G calibration completed the antenna is pointed at the satellite in order to measure the received signal power. Figure 5 illustrates the resulting rf power spectrum as it appears at the LNA input. In this example, the spectrum has a sloping noise baseline with the satellite signal appearing at the center frequency f_o. The shaded areas depict those frequencies passed by the limiting i-f bandpass filter in the ETMS when the ET downconverter is tuned to f_-, f_o or f_+ respectively. The corresponding i-f powers P_-, P_o, and P_+ detected by the ETMS are related to this i-f power spectrum by the equation

$$P_i = \int w(f)\, g_i(f)\, df \qquad (i = -,o,+) \tag{8}$$

where i indicates that the downconverter has been tuned to f_-, f_o or f_+ respectively.

The procedure for normalizing these powers is different from the normalization procedure used in the T_a/G calibration, but is still done for the same purpose, to eliminate gain fluctuations. As previously discussed in the T_a/G measurement with the radio-star, y_1, y_2, and y_3 are calculated from pairs of power measurements with one member of each pair having the solid-state noise source turned on. With reference to figure 4, the magnitude of the added noise power P_a was large enough compared to the $P_i (i = 1,2,3)$ that when P_i was subtracted from the measured power $P_i + P_a$ to obtain P_a significant figures were not lost. However, in the measurement of satellite power (figure 5), P_o and sometimes P_- and P_+, are sufficiently large compared to P_a to cause significant variation in the P_a determined from subtracting $P_i (i = -,o,+)$ from $P_i + P_a$. This problem is circumvented by pointing the ET antenna away (in azimuth) from the satellite to obtain P_a (at f_-, f_o and f_+) by measuring a noise baseline comparable in magnitude to the noise baseline in figure 4, and then normalizing $P_i (i = -,o,+)$ with the resulting P_a's. These P_a's are related to $T_a(f)$ and the receiver gain g(f) by the equation

$$P_{ai} = \int kT_a(f)\, g_i(f) df \qquad (i = -,o,+) \tag{9}$$

where the subscript i signifies whether the ET downconverter has been tuned to f_-, f_o, or f_+.

The ratio difference ΔY of the received satellite signal at the LNA input is calculated from the equation

$$\Delta Y = y_o - (y_- + y_+)/2. \tag{10}$$

With the Δy's of this equation replaced by their theoretical counterparts, equation (1) can be derived. Like the k_i's of equation (7), the e_i's are defined in such a manner as to obtain the functional form of equation (1). As in the T_a/G measurement, the utility of the radio-star method for measuring EIRP depends upon the e_i's being close to unity. The working equations for the e_i's used in the ETMS are to be found in the Appendix.

In obtaining equation (1) from equation (10) a brief explanation of how the aspect angle correction A is defined in this analysis is helpful. Figure 6 depicts a satellite signal being radiated to an earth terminal located in the direction of the spherical angles represented by ω from the center of the mainbeam of the satellite antenna. The spectral power p(f) of the signal available at the output port of the satellite transmitter (TXR) is fed to the satellite antenna whose gain in the ω-direction is $g_s(\omega,f)$. The resulting intensity $I(\omega,f)$ radiated into the infinitesimal solid angle $d\omega$ is

$$I(\omega,f) = p(f)\, g_s(\omega,f) \quad . \tag{11}$$

The aspect angle correction A is then defined in terms of this radiated intensity by the equation

$$A \equiv \frac{\int I(\omega,f)df}{\int I(0,f)df} \tag{12}$$

where $I(0,f)$ is the intensity radiated in the boresight direction of the satellite antenna, and the integrals are evaluated across a narrow bandwidth centered on the center frequency f_o of the signal. The denominator of equation (12) is the EIRP. The ratio in equation (12) reduces with negligible error to the normalized power pattern of the satellite antenna at the center frequency f_o.

III. ERROR ANALYSIS

Examination of equations (1) and (7) reveals that there are twenty-one possible sources of systematic EIRP error. However, since Δy and ΔY, and the e_i's and k_i's are related, the number of sources reduces to thirteen. These thirteen sources of error are listed in the first column of Table I. This table was prepared for an earth terminal operating at 7.55 GHz with an 18 meter antenna looking at a synchronous satellite at 12° elevation above the horizon. The source magnitudes and uncertainties listed in column two reflect this choice. The error in EIRP resulting from the various uncertainties are listed in the third column. Typical random errors generated during T_a/G and received satellite power measurements are given in rows 14 and 15.

The Y-factor ratio uncertainty (0.029 dB) is calculated from the ratio of Δy appearing in equation (4) to the ΔY appearing in equation (10), although the 10 dB magnitude applies to Y only. The uncertainty is mainly due to calibration errors in the i-f attenuators in

the ETMS, the errors due to the power bridge being considerably smaller.

The Cassiopeia A flux-density uncertainty (26 fu) (fu stands for flux units, one flux unit being equivalent to 10^{-26} watts m^2/Hz/steradian) represents a careful but not quite state-of-the-art flux density calibration [9]. This uncertainty and the corresponding 4.46% EIRP error appears difficult to reduce at the present time.

The 0.006 dB uncertainty in the space loss is due to range (r of figure 6) uncertainty which was assumed to be the daily range variation of the satellite used in the example.

The composite ET receiving system-ETMS noise bandwidth is determined at each earth terminal from previously measurement parameters of the ETMS filters and the gain slope of the ET passband.

The uncertainties listed in rows 5 through 11 were calculated from the k_i/e_i ratios for i equal to 1 to 7 respectively. Most of the ratios shown in column 2 are unity because like correction factors tend to cancel each other. The exception is the star-shape correction factor ratio (0.899) where e_2 is always unity because the satellite subtends a vanishingly small solid angle at the ET antenna, and the radio-star does not.

The atmospheric transmission error (7.02%) varies with elevation angle, giving the total EIRP error a characteristic shape shown in figure 7. Table I is a breakdown of this curve at 12° elevation angle. Uncertainties in the k_1/e_1 ratio arise mainly from unpredictable variation in the atmospheric temperature pressure, and water-vapor density profiles between the T_a/G and received satellite power measurements. The large magnitude of this error (7.02%) is due in great part to a lack of measurement data and analysis concerning the tropospheric scattering effect [6,8]. The error could probably be reduced with even a modest effort in this area.

The basis for errors 6 and 7 have been previously discussed [6].

The error due to downlink noise temperature variations includes uncertainties arising from cosmic background variation around the calibrated radio star, and from portions of the satellite signal (if the signal carrier is modulated) appearing in the f_- and f_+ frequency bands (see figure 5) reserved for the baseline noise measurements. The satellite signal was assumed to be unmodulated for these calculations, accounting for the small 0.01% error.

The 1.31% error from antenna pointing inaccuracies is essentially twice the value when pointing at either the radio-star or satellite, and is calculated using an assumed pointing uncertainty of 5% of the antenna half-power-beamwidth.

The polarization mismatch error was calculated assuming axial ratios for the ET and satellite antennas of 0.5 dB and 0.05 dB respectively.

The time constant of the ETMS is sufficiently short and causes no appreciable EIRP error. The 0.23% error in row 11 is due entirely to the T_a instability.

The normalized power pattern of the satellite transmit antenna is needed to determine the aspect angle correction. The 5.29% EIRP error is the result of an aspect angle uncertainty obtained from the literature [1]. The application of emerging spherical near-field scanning techniques [10,11] to satellite antenna measurements should significantly reduce this error.

The quadrature sum of the systematic errors in table I is 10.1%, and is dominated by errors resulting from uncertainties in the Cassiopeia A flux density, the atmospheric transmission factor, and the aspect angle correction. Representative values for the random errors generated during the measurement of T_a/G and received satellite power increase this quadrature error to 18.5%.

The working equations used in the ETMS for measurement and error calculations are found in the Appendix.

IV. CONCLUSIONS

The measurement of EIRP as performed by the ETMS has been described, and an outline of the derivation of the equations leading to the error analysis presented. The results of this analysis are given in table I and figure 7.

The results show a 10% quadrature systematic EIRP error for a 12° elevation angle, increasing to 19% (3σ) with addition of the random errors generated during the measurement.

At 12° elevation angle the total systematic error is dominated by errors resulting from uncertainties in the radio-star flux density, the atmospheric transmission factors, and the aspect angle correction. It appears that the latter two uncertainties might be significantly reduced with presently available knowledge and measurement techniques.

V. ACKNOWLEDGMENTS

The principle support for this work has come from the U.S. Army Communications Command, Fort Huachuca, Arizona 85613, and is gratefully acknowledged.

The Author would also like to thank Dan Bathker and Art Freiley of the Jet Propulsion Laboratories, and Tom Bremer, Moto Kanda, Dave Wait, and John Wakefield of the NBS Laboratories for a number of helpful discussions.

VI. REFERENCES

[1] Steinbrecher, E. E., and Gray, L. F., A computer controlled satellite signal monitoring system, COMSAT Technical Review 1, No. 1 (Fall 1971).

[2] Stelzried, C. T., The JPL total power and noise adding radiometers, NBS High Frequency and Microwave Noise Seminar, unpublished note (May 1970).

[3] Larsen, N. T., and Clague, F. R., The NBS type-II power measurement system, 1970 ISA Annual Conference Proceedings (Philadelphia, Pa.) Paper No. 712-70 25, Part 3 (Oct. 1970).

[4] Kanda, M., An improved solid state noise source, MTT Symposium Digest, Cherryhill, N.J. (June 1976).

[5] Satellite communications reference data handbook, Defence Communications Agency (July 1972).

[6] Daywitt, W. C., Error equations used in the NBS precision G/T measurement system, NBS Internal Note 76-842 (Sept. 1976).

[7] Kraus, J.D., Radio astronomy, (McGraw-Hill Book Co., New York, N.Y., 1966).

[8] Yokoi, H., Yamada, M., and Satoh, T., Atmospheric attenuation and scintillation of microwaves from outer space, Astronomical Society of Japan 22, No. 4, p. 511 (1970).

[9] Kanda, M., An error analysis for absolute flux density measurements of Cassiopeia A, IEEE Trans. I&M, IM-25, No. 3, p. 173 (Sept. 1976).

[10] Wacker, P. F., and Newell, A. H., Advantages and disadvantages of planar, circular cylindrical, and spherical scanning and description of the NBS antenna scanning facilities, from a Workshop on Antenna Testing Techniques sponsored by the European Space Research and Technology Center of the European Space Agency, Noordwijk, Netherlands (June 6-8, 1977).

[11] Larsen, F. H., Probe correction of spherical near-field measurements of a satellite model, from a Workshop on Antenna Testing Techniques sponsored by the European Space Research and Technology Center of the European Space Agency, Noordwijk, Netherlands (June 6-8, 1977).

[12] VanVleck, J. H., The absorption of microwaves by uncondensed water vapor, Phys. Rev. 71, pp. 425-433 (April 1947).

[13] VanVleck, J. H., Theory of absorption by uncondensed gases, Propagation of Short Radio Waves, pp. 646-664 (McGraw-Hill Book Co., Inc., New York, N.Y., 1951).

[14] Bean, B. R., and Dutton, E. J., Radio meteorology, NBS Monogr. 92, 271 pages (March 1966).

[15] Bean, B. R., Cahoon, B. A., Sampson, C. A., and Thayer, G. O., A world atlas of atmospheric radio refractivity, ESSA Monograph 1 (1966).

[16] Valley, S. L. (Editor), Handbook of geophysics and space environments, Air Force Cambridge Research Laboratories, Office of Aerospace Research, United States Air Force (1965).

[17] Daywitt, W. C., Atmospheric corrections used in the NBS earth terminal measurement system, NBSIR (to be published, Fall 1977).

[18] Baars, J. W. M., Mezger, P. G., and Wendker, H., The spectra of the strongest non-thermal radio sources in the centimeter-wavelength range, Astrophysical J. 142, pp. 122-134 (1965).

[19] Raghava Rao, R., Medd, W. J., Higgs, L. A., and Broten, N. W., Survey of 9.4 cm radio emission in Cassiopeia and Cepheus, Royal Astronomical Society Monthly Notices 129, No. 2, p. 159 (1965).

[20] Dent, W. A., Aller, H. D., and Olsen, E. T., The evolution of the radio spectrum of Cassiopeia A, Astrophysical J. 188, L 11 (Feb. 1974).

VII. APPENDIX: MEASUREMENT AND ERROR EQUATIONS

The ETMS computer software contains a number of simplified working equations for calculating the parameters found in equations (1) and (7), and the various EIRP errors appearing in table I. These equations are collected here with an indication of the references upon which they are based, but with little or no further comment. The equations were derived for the 1 to 10 GHz frequency range, and do not necessarily apply outside of this range.

A. T_a/G Correction Factors - k_i

Although these correction factors are defined in precisely the same way as the G/T correction factors with corresponding working equations previously appearing in the literature [6], a number of the equations have undergone improvements since that time. Therefore, these correction factors will be listed here again. The corresponding errors $E(k_i)$ are included for completeness, and are used in determining the G/T or T_a/G errors only, not the EIRP errors. EIRP correction-factor errors are calculated from k_i/e_i ratios, and appear in a later section of this Appendix.

1. Atmospheric Transmission Factor - k_1

$$k_1 = k_g\, k_r\, k_d \quad .$$

1.1 Gaseous Absorption Factor - k_g

$$k_g = 10^{-A_g \,\mathrm{Csc}\,\theta/10} \quad .$$

$$A_g = \gamma_1 \ell_1 + \gamma_2 \ell_2 + \gamma_3 \ell_3 \,(\mathrm{dB}).$$

θ = ET antenna elevation angle $\geq 3°$

$$\gamma_1 = 6.644 \times 10^{-3} (P_o/P_S)^2 \left(\frac{T_o}{T}\right)^{2.75} (1+0.02215ZT_o/T)^{-10.52} \cdot \left(\frac{0.9211}{1+0.2912/f^2} + \frac{5.107(1+3596/f^2)}{(1-3596/f^2)^2}\right) \left(\frac{\mathrm{dB}}{\mathrm{km}}\right) \quad .$$

$$\ell_1 = 5.145 \left(\frac{T}{T_o}\right) \left\{1 - \left[1-0.02215(11.02-Z)\,\frac{T_o}{T}\right]^{8.775} + 4.29\left[1-0.02215(11.02-Z)\frac{T_o}{T}\right]^{7.775}\right\}$$

$$+ (1.047-0.09502Z)\left[1-0.02215(11.02-Z)\,\frac{T_o}{T}\right]^{7.775} \ (\mathrm{km}) \quad .$$

$$\gamma_2 = 1.451 \times 10^5 (P_o/P_S) \quad \frac{e^{-644/T}}{T^3} \left(1+0.02215Z \frac{T_o}{T}\right)^{-5.262}$$

$$\cdot \left(\frac{1+493.3/f^2}{(1-493.3/f^2)^2}\right) \rho(1+0.0046\rho) \quad \left(\frac{dB}{km}\right) \quad .$$

$$\ell_2 = 2.09 + 0.27\left(1- \frac{T_o^2}{T^2}\right) \quad (km) \quad .$$

$$\gamma_3 = 2.529 \times 10^{-2} (P_o/P_S) \quad \frac{f^2}{T^{1.5}} \left(1+0.02215 \; Z \frac{T_o}{T}\right)^{-5.262}$$

$$\cdot \rho(1+0.0046\rho) \left(\frac{dB}{km}\right) \quad .$$

$\ell_3 = 2.17$ (km) .

Z = ET antenna altitude above sea level (km).

T_o = 293 (kelvins).

T = Air temperature at ET antenna (kelvins).

P_S = 1013.25 m bar

P_o = Reduced-to-sea-level value of atmospheric pressure at ET antenna in m bar.

ρ = Water-vapor density at ET antenna (gm/m^3).

The error in k_g is

$$E(k_g) = 50(k_g^{-1}-1) \quad (\%)$$

This error includes contributions from uncertainties in the constants appearing in $\gamma_1, \gamma_2, \gamma_3, \ell_1, \ell_2$, and ℓ_3; the earth-terminal altitude; atmospheric temperature and water-vapor density profiles; the csc θ approximation; termination of the calculation at 20 km from ground level into the atmosphere; and ET antenna pointing errors.

1.2 Refractive Spreading Factor - k_r

1.2.1 Gaussian Main Beam With a Disk Source

$$k_r = 1 + \left(\frac{x^2}{e^{x^2}-1}\right) \frac{\partial \tau}{\partial \theta} \quad .$$

$$- \frac{\partial \tau}{\partial \theta} = \frac{\pi \; (B - 0.026 \; \text{Ctn} \; \theta) \text{Csc}^2 \theta}{60 \times 180} \quad .$$

$$x = \frac{\text{Star diameter (4.6' for Cas A)}}{1.2 \; (\text{HPBW})} < 1 \; .$$

HPBW = Half-power-beamwidth (Same units as star diameter).

$$B(\theta \geq 3^\circ) = \frac{T_o}{T}\left[0.9227(1 - 0.02252Z)^{5.262} + 0.0202\rho\right] \operatorname{Ctn} \theta .$$

$$E(k_r) = 18(k_r^{-1} - 1) \ (\%) .$$

1.2.2 Gaussian Main Beam With an Elliptical Gaussian Source

$$k_r = 1 + k_2\left(\frac{\partial \tau}{\partial \theta}\right) .$$

k_2 = k_2 factor for an elliptical gaussian source (equation appears later).
$E(k_r)$ equation is assumed to be identical with the previous $E(k_r)$ equation.
This error includes uncertainties in ET antenna pointing, and the refraction angle correction for antenna pointing (see below).

The ET antenna elevation angle θ differs from the true elevation angle to the extra-terrestial source (satellite or radio-star) by a refraction correction τ. The working equation for τ derived for the computer software is ($\theta \geq 3^\circ$)

$$\tau = 0.952 \frac{T_o}{T}\left[\frac{P_o/P_s}{(1+0.0221SZT_o/T)^{5.262}} + 0.0219\rho\right]\operatorname{ctn}\theta$$

$$- 0.0135 \operatorname{ctn}^2 \theta \text{ (arcminutes)}.$$

$$E(\tau) = 0.2 \operatorname{ctn} \theta \text{ (arcminutes)}.$$

This error includes uncertainties from the approximate nature of the τ working equation, the elevation angle θ, ET antenna altitude, and atmospheric temperature, pressure, and water-vapor density profiles.

1.3 Tropospheric Scattering Factor - k_d

$$k_d = 1 + \left(\frac{x^2}{e^{x^2}-1}\right)\left(10^{A_d \operatorname{Csc}\theta/10} - 1\right) .$$

$$A_d = 0.0011 f^2 \text{ (dB)}.$$

$$E(k_d) \equiv 75(k_a^{-1} - 1) \ (\%).$$

This error represents only an educated guess because of the present inavailability of a more exact equation describing the energy lost by scattering of an extra terrestrial radio wave as it traverses the atmosphere to the ET antenna.

The primary references upon which the preceeding equations are based are 6, 8, 9, 12, 13, 14, 15, 16, and 17.

2. Star Shape Correction Factor - k_2

For a gaussian mainbeam,

$$k_2 = \frac{1-e^{-x^2}}{x^2} \quad \text{(disk source)}$$

$$= \left[1 + \frac{D_1^2}{\theta_H^2}\right]^{-1} \left[1 + \frac{D_2^2}{\theta_H^2}\right]^{-1} \quad \text{(elliptical gaussian source).}$$

D_1 = major half-power diameter of source.

D_2 = minor half-power diameter of source.

$E(k_2) = 6(1-k_2) + 0.10$ (%).

This error includes uncertainties from the approximate nature of the k_2 equation, uncertainties in the Cas A disk diameter, and uncertainties in the ET antenna HPBW determined by the ETMS. The error was derived for this disk source and is assumed to hold for the gaussian source.

The pertinent references for k_2 are 6, 9, 17, and 18.

3. Bandwidth Factor - k_3

$$k_3 = 1 \pm 0.00\% \ .$$

4. Differential System Noise Temperature Factor - k_4

$$k_4 = 1.$$

$$E(k_4) = \frac{0.4\ \overline{T}\ \theta_H^2}{S} \quad (\%) \ .$$

$\overline{T}$ = Average noise temperature of the cosmic background surrounding the radio star (= 1 kelvin for CAS A).

θ_H = ET antenna HPBW (arcminutes).

S = Radio star flux density (f.u.).

The pertinent references for k_4 are 6 and 19.

5. Antenna Pointing Factor - k_5

$$k_5 = 1.$$

$$E(k_5) = 0.028\ \varepsilon^2 \ (\%).$$

ε = ET antenna pointing error as a percent of the antenna HPBW.

The pertinent references for k_5 are 6 and 9.

6. Polarization Factor - k_6

$$k_6 = 1.$$

$$E(k_6) = d \cos 2\varepsilon_a \ (\%).$$

$\varepsilon_a = \mathrm{Ctn}^{-1}(AR_a)$.
AR_a = ET antenna axial ratio.
d = Radio-star polarization (%).

The pertinent references for k_6 are 6 and 9.

7. System Response Factor - k_7

$$k_7 = 1 \pm 0.00\%.$$

The pertinent references for k_7 is 6.

B. Radio-Star Flux Density - S

$S = S_o e^{a\Delta t} f^{\alpha_o + b\Delta t}$.
S_o = 3154 f.u. ± 4.46%.
$a = -0.0097 \pm 0.0005 \ (yr^{-1})$.
$b = +0.00126 \pm 0.00023 \ (yr^{-1})$.
$\alpha_o = -0.792 \pm 0.006$.
Δt = Epoch - 1965.0.
$E(S) = 4.46 + 0.050\,\Delta t + 0.602\,\ell n(f) + 0.023\,\Delta t\,\ell n(f)$ (%).

The value used for S_o was obtained from an unpublished Jet Propulsion Laboratory measurement performed at 2.2785 GHz in 1972.6, and extrapolated to 1 GHz using the Dent-Aller-Olsen equation [20]. The error for S_o was derived from reference 20.

C. ΔY-Factor Ratio Differences - Δy, ΔY

The equations for the ratio differences Δy and ΔY are given in the text. The error for the ratio ΔY/Δy is

$$E(\Delta Y/\Delta y) = 0.66\%.$$

D. Noise Bandwidth - Δf

$\Delta f = \Delta f_o(1 + bN_1)$ (MHz).
Δf_o = ETMS noise bandwidth (MHz).
= 1.193* (MHz).
N_1 = ETMS filter constant
= - 0.010 (MHz).
$E(\Delta f) = 0.38$ (%).
b = i-f gain slope of the ET spectrum around the signal frequency (MHz^{-1}).
*These values differ from filter to filter and are given here only for illustration.

E. Space Loss - L

$$L = \left(\frac{4\pi r}{\lambda}\right)^2 .$$

r = slant range (see figure 6) from ET antenna to satellite.

λ = Signal wavelength.

The pertinent reference for L is 5.

F. Aspect Angle Correction - A

A = Normalized power pattern of satellite antenna in the direction of the earth terminal.

E(A) = 5.92 (%) (0.25 dB).

This error was obtained from reference 1.

G. EIRP Correction Factors - e_i

1. Atmospheric Transmission Factor - e_1

$$e_1 = e_g\, e_r\, e_d .$$

1.1 Gaseous Absorption Factor - e_g

Same equation as that used for k_g.

$$E(k_g/e_g) = 60(e_g^{-1}-1)\ (\%).$$

Note that in the EIRP measurement, correction factor errors are calculated from the ratios k_i/e_i because the k_i and e_i are related. In this and the next two errors only atmospheric profile changes between the T_a/G and satellite received power measurements cause significant errors.

1.2 Refractive Spreading Factor - e_r

Same equation as that used for k_r with x = 0.

$$E(k_r/e_r) = 26(e_r^{-1}-1)(\%).$$

1.3 Tropospheric Scattering Factor - e_d

Same equation as that for k_d with x = 0.

$$E(k_d/e_d) = 90(e_d^{-1}-1)\ (\%).$$

2. Star Shape Factor - e_2

$$e_2 = 1 \pm 0.00\%.$$

3. Bandwidth Factor - e_3

$$e_3 = 1.$$

$$E(k_3/e_3) = 0.0058p \ (\%).$$

p = Percentage of i-f passband occupied by received satellite signal.

4. Differential Operating Noise Temperature Factor - e_4

$$e_4 = 1.$$

$$E(k_4/e_4) = \frac{0.4\ \bar{T}\ \theta_H^2}{S} + 25\ \left(\frac{P'_- + P'_+}{T}\right)\ (\%) \quad .$$

P'_- = Signal power contained in the frequency band (see figure 5) reserved for the lower frequency (f_-) noise measurement.

P'_+ = Signal power contained in the frequency band (see figure 5) reserved for the upper frequency (f_+) noise measurement.

T = Operating noise temperatures (see text).

5. Antenna Pointing Factor - e_5

$$e_5 = 1.$$

$$E(k_5/e_5) = 0.055\ \varepsilon^2\ (\%) \quad .$$

6. Polarization Factor - e_6

$$e_6 = 1.$$

$$E(k_6/e_6) = d \cos 2\ \varepsilon_a + 100 \sin^2(\varepsilon - \varepsilon_a) + 100 \cos 2\varepsilon \cos 2\varepsilon_a\ (\%) \quad .$$

$$= 0.11d + 0.40\ (\%)$$

$\varepsilon = \text{ctn}^{-1}(AR)$.

$\varepsilon_a = \text{ctn}^{-1}(AR_a)$.

AR = Satellite antenna axial ratio in the ET antenna direction (0.05 dB was used for AR, and 0.5 dB was used for AR_a).

The pertinent reference for e_6 is 9.

7. System Response Factor - e_7

$$e_7 = 1.$$

$$E(k_7/e_7) \doteq E(e_7) = \frac{\Delta T_a}{T_a} = 0.23\% \quad .$$

T_a = Noise temperature of the solid-state noise source as it appears at the LNA input.

ΔT_a = Maximum possible change in T_a between the T_a/G and received satellite power measurements.

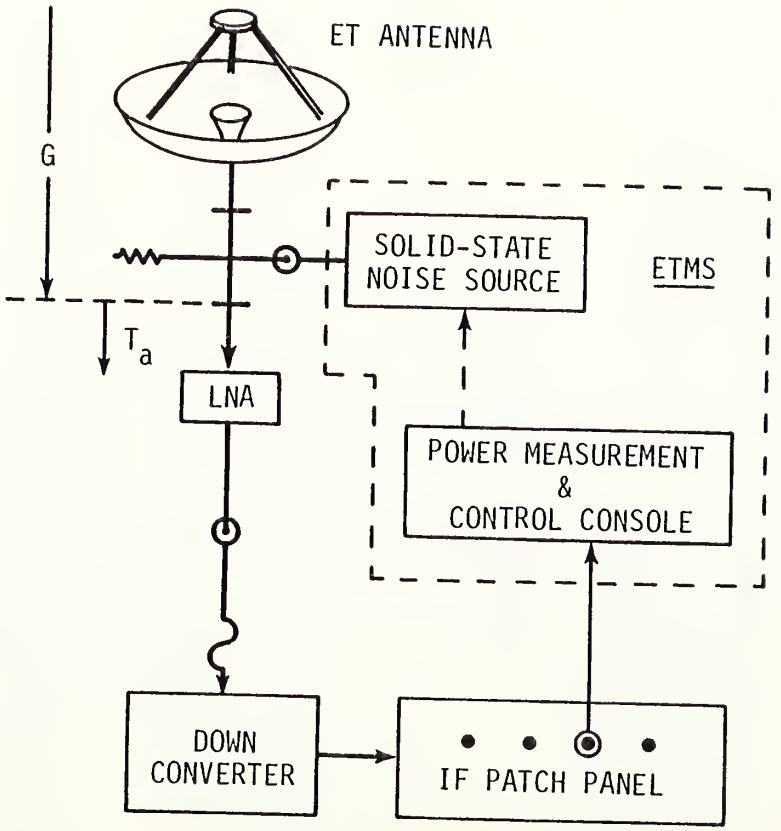

Figure 1. Interface between the earth terminal measurement system and the earth-terminal receiving system.

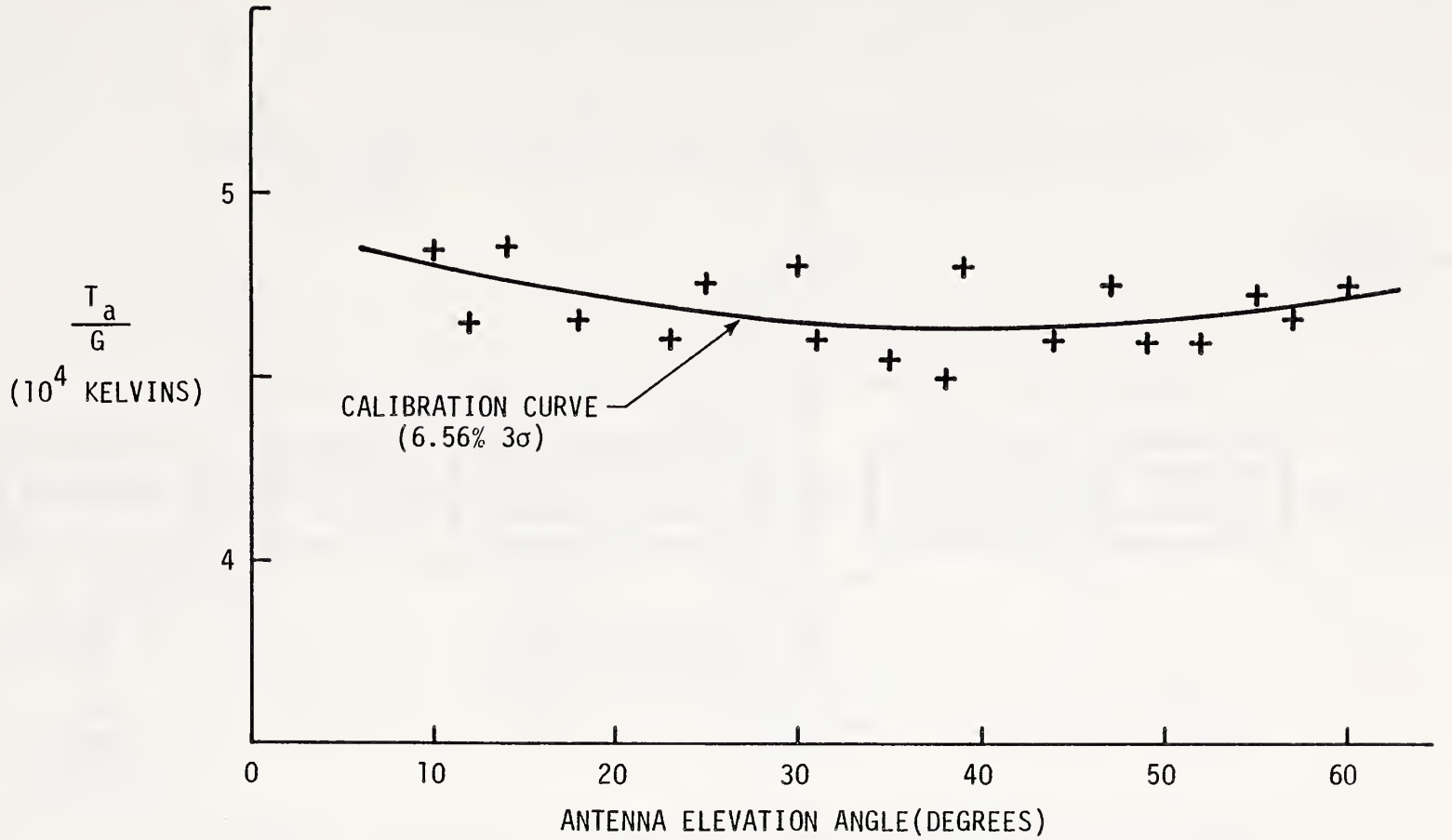

Figure 2. T_a/G earth-terminal calibration curve.

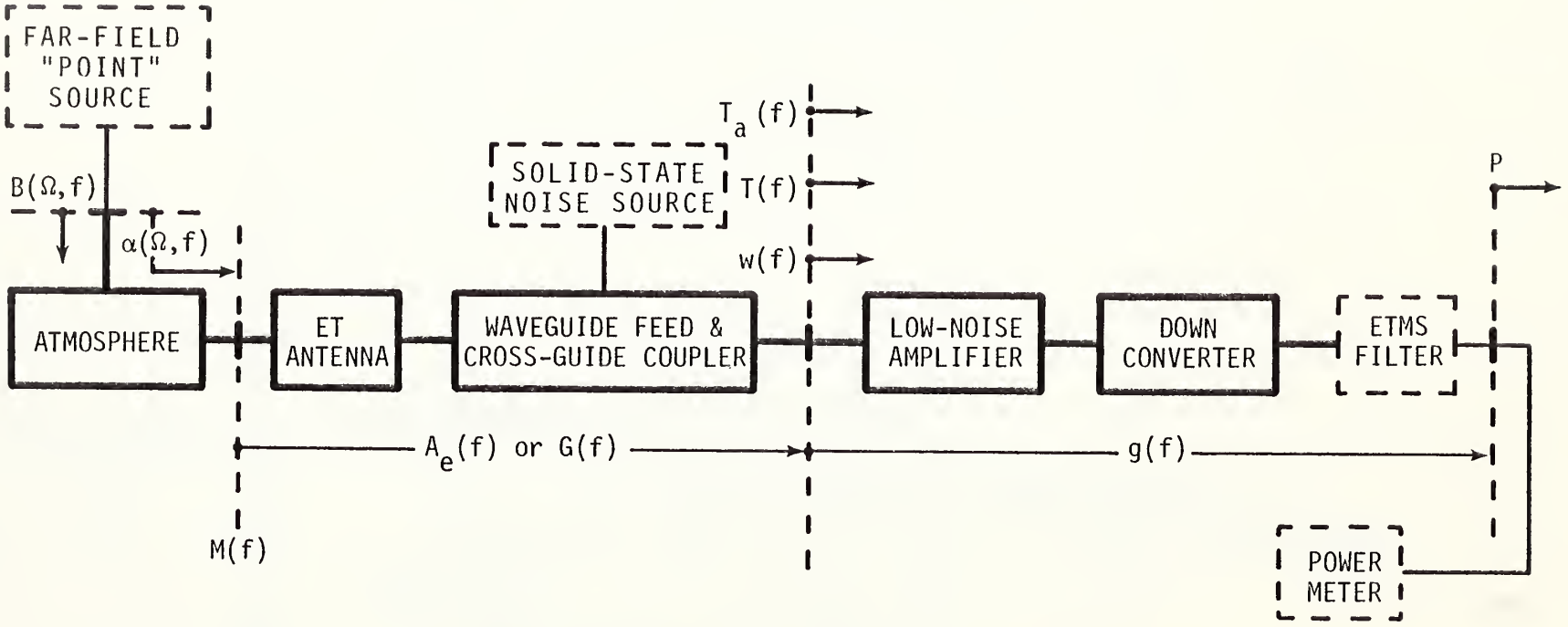

Figure 3. Block diagram of a model representing the earth-terminal receiving system.

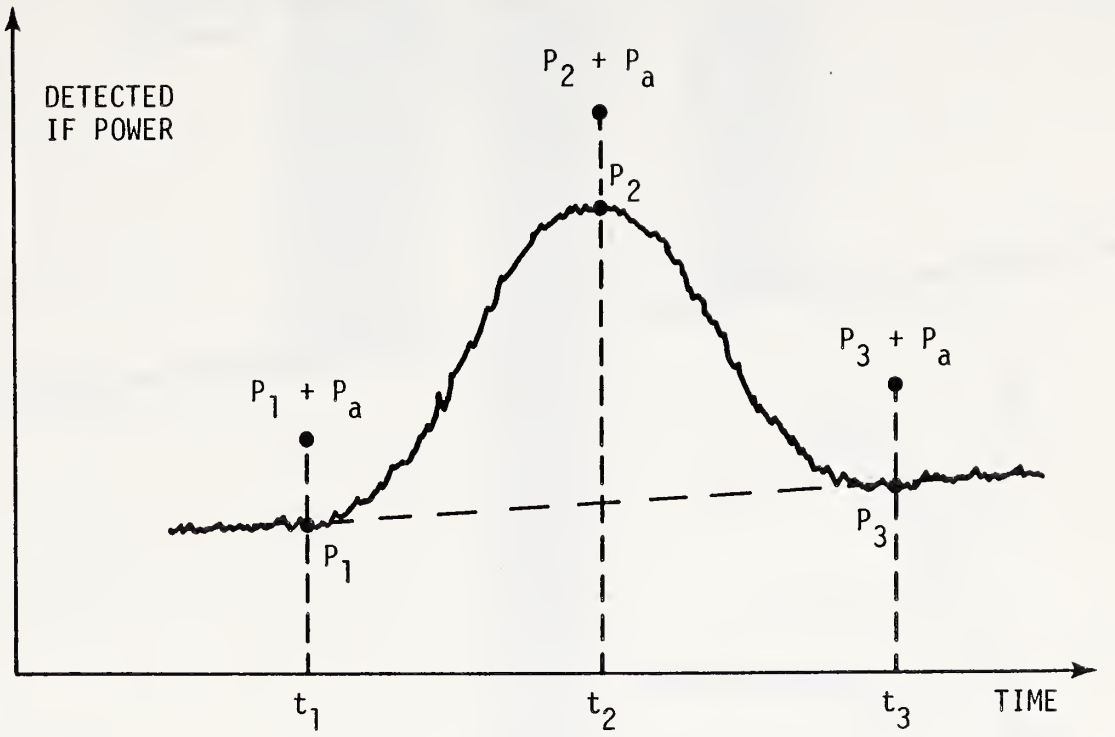

Figure 4. IF power detected by the earth terminal measurement system as a radio star traverses the earth-terminal antenna mainbeam.

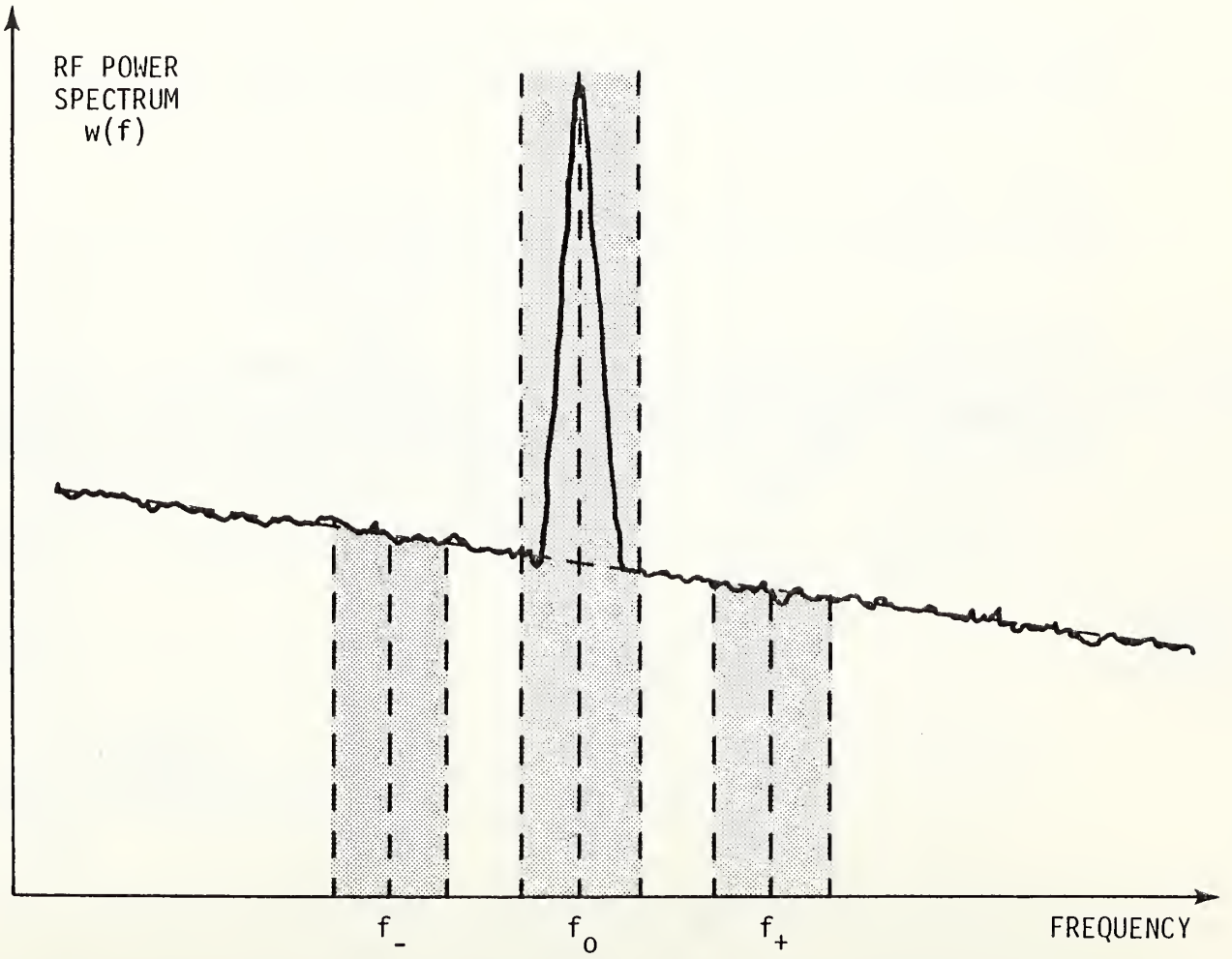

Figure 5. A portion of the RF power spectrum as it appears at the low-noise amplifier input.

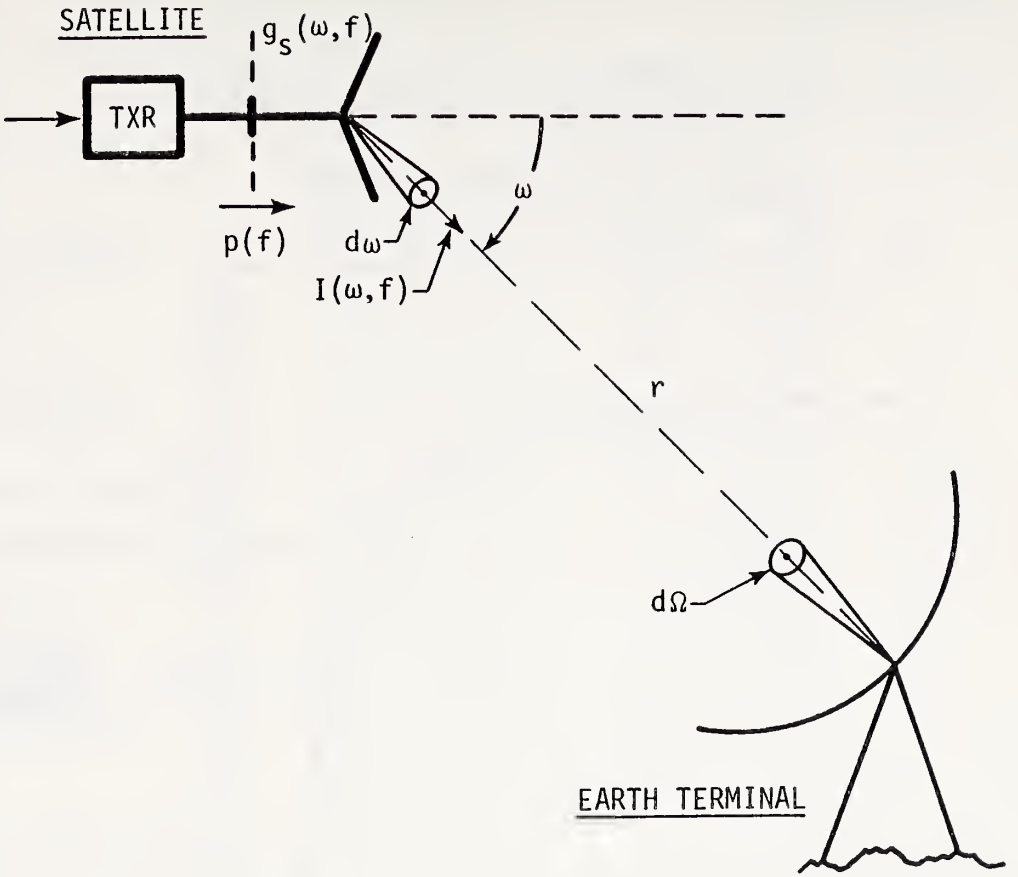

Figure 6. Parameters used in the definition of satellite EIRP and the resulting power flux at the earth-terminal antenna aperture.

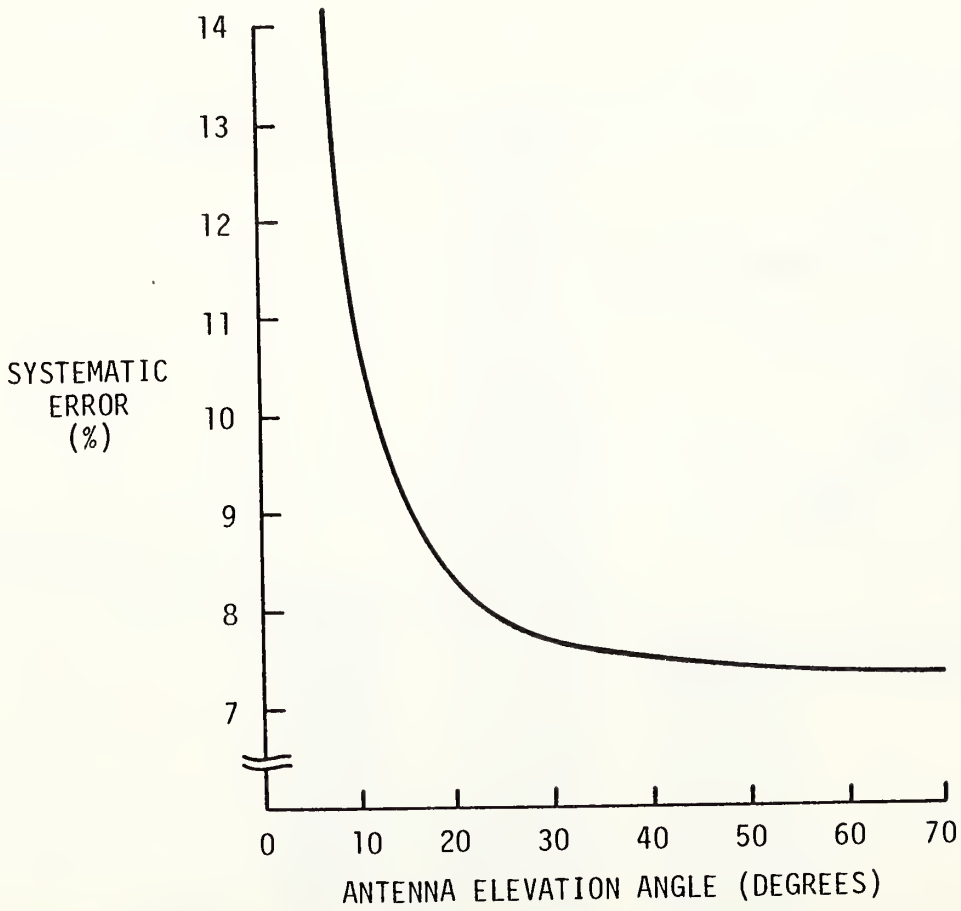

Figure 7. Total quadrature systematic EIRP error at 7.55 GHz versus earth-terminal antenna elevation angle.

TABLE I.

ERROR IN MEASURING EIRP AT 7.55 GHZ & 12° ELEVATION ANGLE

SOURCE OF ERROR	SOURCE MAGNITUDE AND UNCERTAINTY	RESULTING PERCENT ERROR IN EIRP
1. Y-Factor Ratio	10 ± 0.029 dB	0.66
2. Cassiopeia A Flux Density	586 ± 26 fu	4.46
3. Space Loss $(4\pi r/\lambda)^2$	202 ± 0.006 dB	0.14
4. Noise Bandwidth	5 MHZ ± 19 kHz	0.38
5. Atmospheric Transmission	1 ± 0.0702	7.02
6. Star Shape	0.899 ± 0.0070	0.81
7. Component Frequency Dependence	1 ± 0.0073	0.73
8. Downlink Noise Temperature Variation	1 ± 0.0001	0.01
9. ET Antenna Pointing	1 ± 0.0131	1.31
10. Polarization Mismatch	1 ± 0.0056	0.56
11. System Time Response & T_a Instability	1 ± 0.0023	0.23
12. Aspect Angle Correction	0 ± 0.25 dB	5.29
13. Frequency	7.55 ± 0.00 GHz	0.00
QUADRATURE SUM OF SYSTEMATIC ERRORS		10.1%
14. Random Error From T_a/G Measurement	-33.2 ± 0.28 dB(3σ)	6.56
15. Random Error From Received Satellite Power	± 0.57 dB(3σ)	14.10
TOTAL QUADRATURE ERROR		18.5%

NBS-114A (REV. 7-73)

U.S. DEPT. OF COMM. BIBLIOGRAPHIC DATA SHEET	1. PUBLICATION OR REPORT NO. NBSIR 78-869	2. Gov't Accession No.	3. Recipient's Accession No.

4. TITLE AND SUBTITLE

ERROR EQUATIONS USED IN THE NBS EARTH TERMINAL MEASUREMENT SYSTEM

5. Publication Date: December 1977

6. Performing Organization Code: 276.05

7. AUTHOR(S): William C. Daywitt

8. Performing Organ. Report No.

9. PERFORMING ORGANIZATION NAME AND ADDRESS

NATIONAL BUREAU OF STANDARDS
DEPARTMENT OF COMMERCE
WASHINGTON, D.C. 20234

10. Project/Task/Work Unit No.: 2765266

11. Contract/Grant No.

12. Sponsoring Organization Name and Complete Address *(Street, City, State, ZIP)*

13. Type of Report & Period Covered

14. Sponsoring Agency Code

15. SUPPLEMENTARY NOTES

16. ABSTRACT *(A 200-word or less factual summary of most significant information. If document includes a significant bibliography or literature survey, mention it here.)*

An outline for the derivation of equations employed in a measurement and error analysis of satellite EIRP using a calibrated radio star is presented. A table showing analysis results at 7.55 GHz using Cassiopeia A for a satellite at 12° elevation angle is given. The quadrature sum of the systematic errors appearing in the table is 10.1%. Also presented is a curve of the systematic errors as a function of elevation angle showing a 7.3% minimum at high elevation angles. Included are working equations for the calculation of correction and errors.

17. KEY WORDS *(six to twelve entries; alphabetical order; capitalize only the first letter of the first key word unless a proper name; separated by semicolons)*

C/kT; EIRP; error analysis; G/T; precision measurements; radio star; satellite communications.

18. AVAILABILITY

[xx] Unlimited

[ ] For Official Distribution. Do Not Release to NTIS

[ ] Order From Sup. of Doc., U.S. Government Printing Office Washington, D.C. 20402, SD Cat. No. C13

[X] Order From National Technical Information Service (NTIS) Springfield, Virginia 22151

19. SECURITY CLASS (THIS REPORT): UNCLASSIFIED

21. NO. OF PAGES: 32

20. SECURITY CLASS (THIS PAGE): UNCLASSIFIED

22. Price: $4.50